

End-Plate Connection Moment–Rotation Relationship

A. R. Kukreti, T. M. Murray and A. Abolmaali

School of Civil Engineering and Environmental Science, University of Oklahoma, Norman,
Oklahoma, USA

SYNOPSIS

A methodology, based on finite element modeling, is presented to analytically develop the moment–rotation relationship for a bolted steel end-plate connection. The methodology is demonstrated for a flush end-plate connection. Experimental testing of a few selected specimens was conducted to verify the finite element modeling and associated computer analysis procedure. The finite element model was used to conduct a parametric study to determine the effect of various geometric and force related variables on the prediction of maximum end-plate separation. Sufficient cases were then analyzed, which cover the variation of these variables within practical ranges. The analyses data collected were regressed to develop a prediction equation characterizing the general behavior of the connection.

NOTATION

b_p	End-plate width.
d_b	Nominal bolt diameter.
g	Gage of the bolts (centerline distance between two bolts).
g_b	Width of equivalent rectangular area to represent the bolts.
h	Beam depth.
n	Total number of beam cross sections selected.
p_t	Pitch of the bolt (distance from top of the flange to the centerline of the bolt).
t_p	End-plate thickness.
t_w	Beam web thickness.
x, y, z	Cartesian global coordinate directions.
A_B	Beam cross-sectional area.

C	Coefficient dependent on end-plate thickness, beam dimensions, bolt diameter and pitch of the tension bolt.
C'	$1/C$
E	Young's modulus of elasticity.
E_s	Secant modulus of elasticity.
F_{by}	Yield stress of beam material.
F_{ub}	Ultimate stress of bolt material.
F_y	Yield stress.
F_{yb}	Yield stress of bolt material.
M	Applied moment on the beam stub.
M_m	Moment-carrying capacity of the m th beam cross section chosen.
M_y	Yield moment capacity of a beam cross section.
$(M_y)_{\max}$	Maximum value of M_y for all the beam cross sections selected.
$(M_y)_{\min}$	Minimum value of M_y for all the beam cross sections selected.
ΔM	$(M_y)_{\max} - (M_y)_{\min}$
R^2	Coefficient of multiple determination for the regression analysis.
S	Elastic section modulus of the beam cross section.
α	Scalar number varying from 0.1 to 1.0 in increments of 0.1 to denote the beam load level.
β	Power of moment, M , in the moment-rotation relationship.
δ	Maximum end-plate separation.
ϵ_{eff}	Effective strain for von Mises yield criterion.
ϵ_y	Yield strain.
$\epsilon_1, \epsilon_2, \epsilon_3$	Principal strains ($\epsilon_1 > \epsilon_2 > \epsilon_3$).
Θ	End-plate connection rotation.
π_1	t_p/h
π_2	p_t/h
π_3	t_w/h
π_4	t_t/h
π_5	b_p/h
π_6	d_b/h
π_7	g_b/h
π_8	Bending stiffness parameter for the end plate.
π_9	M
π_a	δ
Φ	Ratio of the 3-D value of δ to the corresponding 2-D value.

1 INTRODUCTION

Real connections in steel structures are neither perfectly 'rigid' nor perfectly 'flexible'. Even the 'rigid' connections recommended by the American

Institut
On the
used, c
neede
memb
rotatio
tests c
could
nection
gather
(e.g. s
the w
model
bolted
flush e
provic
as sho
Exper
and 1
comp
valida
regre
behav
Co
natur
plate
devel
tee-s
edge
McG
Steel
were
meth
Stru
beer
Kris
the
Bas
figu
met
stuc
con

sions,
sen.
l.
sis.
note

Institute of Steel Construction (AISC) Manual¹ are flexible to some extent. On the other hand, the 'flexible' shear connections, which are commonly used, do transfer some moment. Thus moment-rotation relationships are needed for the analysis and design of steel framed structures for which the members are connected by semi-rigid connections. In the past, moment-rotation curves for some connections were developed from experimental tests conducted on actual connections.^{2,3} But, in general, such a concept could not be extended for other connections since tests of prototype connections are time-consuming and expensive, and above all, the data gathered from tests are few and generally limited to surface measurements (e.g. strain measurements on the surface). As an alternative, in this paper the writers have presented a methodology, based on finite element modeling, to analytically develop the moment-rotation relationship for a bolted steel end-plate connection. To demonstrate this methodology, a flush end-plate connection is considered. Such a connection may be used to provide a connection between two beams, called a 'splice plate connection', as shown in Fig. 1a, or between a beam and a column, as shown in Fig. 1b. Experimental testing of a few selected specimens was conducted to confirm and modify accordingly the finite element modeling and associated computer analysis procedure. Once the computer analysis procedure was validated, a parametric study was conducted and the data collected were regressed to develop prediction equations characterizing the general behavior of the connection.

Considerable research results, of both an analytical and experimental nature, are available for extended end-plate connections, in which the end plate projects beyond the beam flanges. Early attempts (prior to 1970) to develop a design methodology for such end-plate connections were based on tee-stub analogy. In these studies the prying action was assumed to act at the edge of the end plate. One of these methods was developed by Douty and McGuire⁴ and was presented in the seventh edition of the *AISC Manual of Steel Construction*.⁵ Other significant methods using the tee-stub analogy were suggested by Kato and McGuire⁶ and Nair *et al.*⁷ Along with other methods, the aforementioned methods are summarized by Fisher and Struik.⁸ More recently, methods based on refined yield line analyses have been suggested by Zoetemeijer,⁹ Mann and Morris,¹⁰ and Kennedy *et al.*¹¹ Krishnamurthy¹² developed the finite element methodology, specifically for the analysis of unstiffened, four-bolt-extended end-plate connections. Based on finite element analyses of a large number of geometric configurations of the connection, Krishnamurthy developed the design methodology found in Reference 1. From Krishnamurthy's theoretical studies it was found that even though prying action was present, it was overly conservative to assume that the prying action acted at the edge of the plate

ctly
can

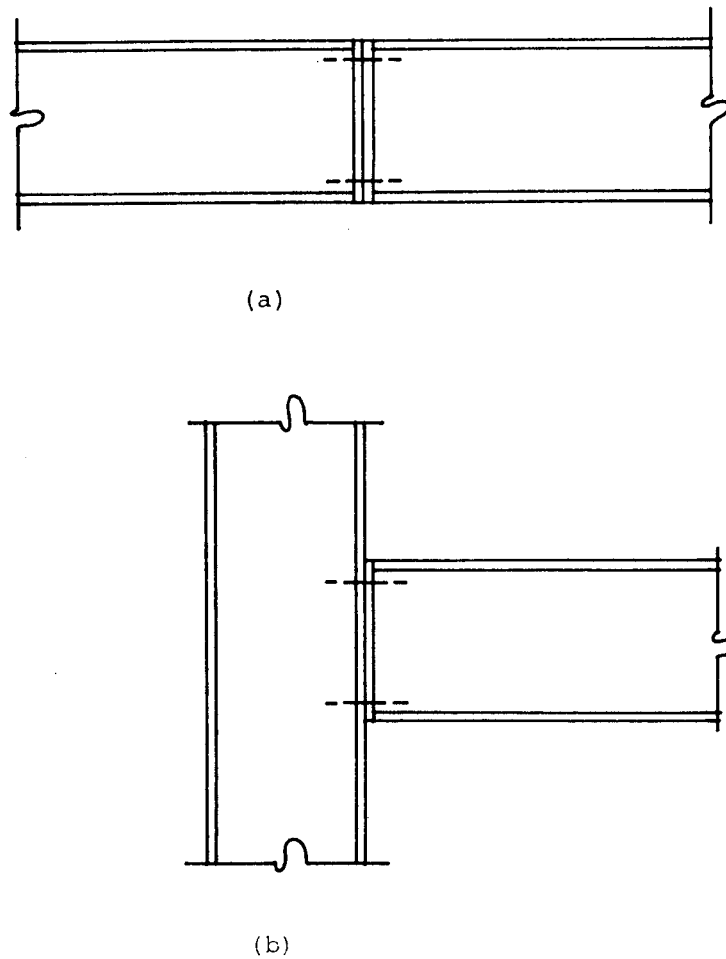


Fig. 1. Typical uses of flush end-plate connections. (a) Beam-to-beam connection (splice connection). (b) Beam-to-column connection.

since it resulted in thicker than necessary plates. Krishnamurthy also investigated the behavior of stiffened tee-stubs¹³ as it applied to the stiffened extended end-plate connections. Tarpay and Cardinal,¹⁴ based on tests and linear finite element analysis, developed a moment-rotation/strength relationship for the unstiffened end-plate connection. The end-plate thickness was described as the 'key parameter' on the response of the connection. Ahuja¹⁵ was the first to investigate stiffened end-plate connections with two rows of bolts on either side of the tension flange. Basically this was an extension of the work done by Krishnamurthy.¹² Based on linear finite element analyses, prediction equations were developed to predict maximum end-plate separation and forces in the bolts. Ghassameih¹⁶ later extended this work to incorporate the non-linear material behavior of the end-plate and the bolt shank material. Hendrick¹⁷ has studied the column strength at the end-plate connections.

Prob
connec
both e
behavi
Morris
analysi
French
capaci
Parker
plate t
collapse
elemen
multip
beam-
used to
results

The f
nectio
Howe
two-c
costly
conn
on a
mid-
stres
relat
analy
cons
prac
resu
expe
A
stud
adeq
web
wid
bolt
sepa

Probably because of its smaller moment capacity, the flush end-plate connection has received much less attention. Douty and McGuire⁴ studied both extended and flush end-plate connections and concluded that the behavior and strength of these two connections differ greatly. Parker and Morris,¹⁸ Blockley,¹⁹ Zoetermeijer²⁰ and Srouji²¹ have presented a yield line analysis procedure for flush end-plate connections. The German²² and the French²³ specifications have presented formulae to determine the moment capacity of the connection for a given flush end-plate thickness. Phillips and Parker²⁴ conducted a series of tests to determine the influence of the end-plate thickness on the moment-rotation characteristics and the end-plate collapse mechanism. Krishnamurthy²⁵ developed the two-dimensional finite element model to predict the behavior of flush end-plate connections with multiple rows of bolts in the tension region. For other types of bolted beam-to-column connections finite element methods have been successfully used to model the connection behavior when compared to experimental test results, for example, refer to Reference 26.

2 ANALYTICAL MODELING

The finite element method was used to analyze the flush end-plate connection. The problem is obviously three-dimensional (3-D) in nature. However, a 3-D finite element analysis is much more complicated than a two-dimensional (2-D) analysis, and above all, computationally much more costly. To develop prediction equations characterizing the behavior of the connection, it was therefore decided to conduct 2-D finite element analysis on a plane stress model taken parallel to the plane passing through the mid-thickness of the web. Since transverse variations of deformations and stresses cannot be represented in this model, in order to determine the relationship that exists between the 2-D and 3-D results, 3-D finite element analyses were conducted on certain 'bench mark' connections which are considered representative of common fabrication and construction practices. A correlation factor was then developed between the 2-D and 3-D results to enable the prediction of the more accurate 3-D values from the less expensive 2-D results.

A typical configuration of the 2-D finite element model used in the present study is shown in Fig. 2. A length of the beam equal to its depth is chosen as adequate for inclusion in the analysis domain. The end plate, beam flanges, web and bolt shank are represented as plane stress elements, with their width equal to their thicknesses measured perpendicular to the web. The bolts near the tension flange are simulated by modeling the bolt shanks as separate elements, connected to the end-plate nodes at the plate surface,

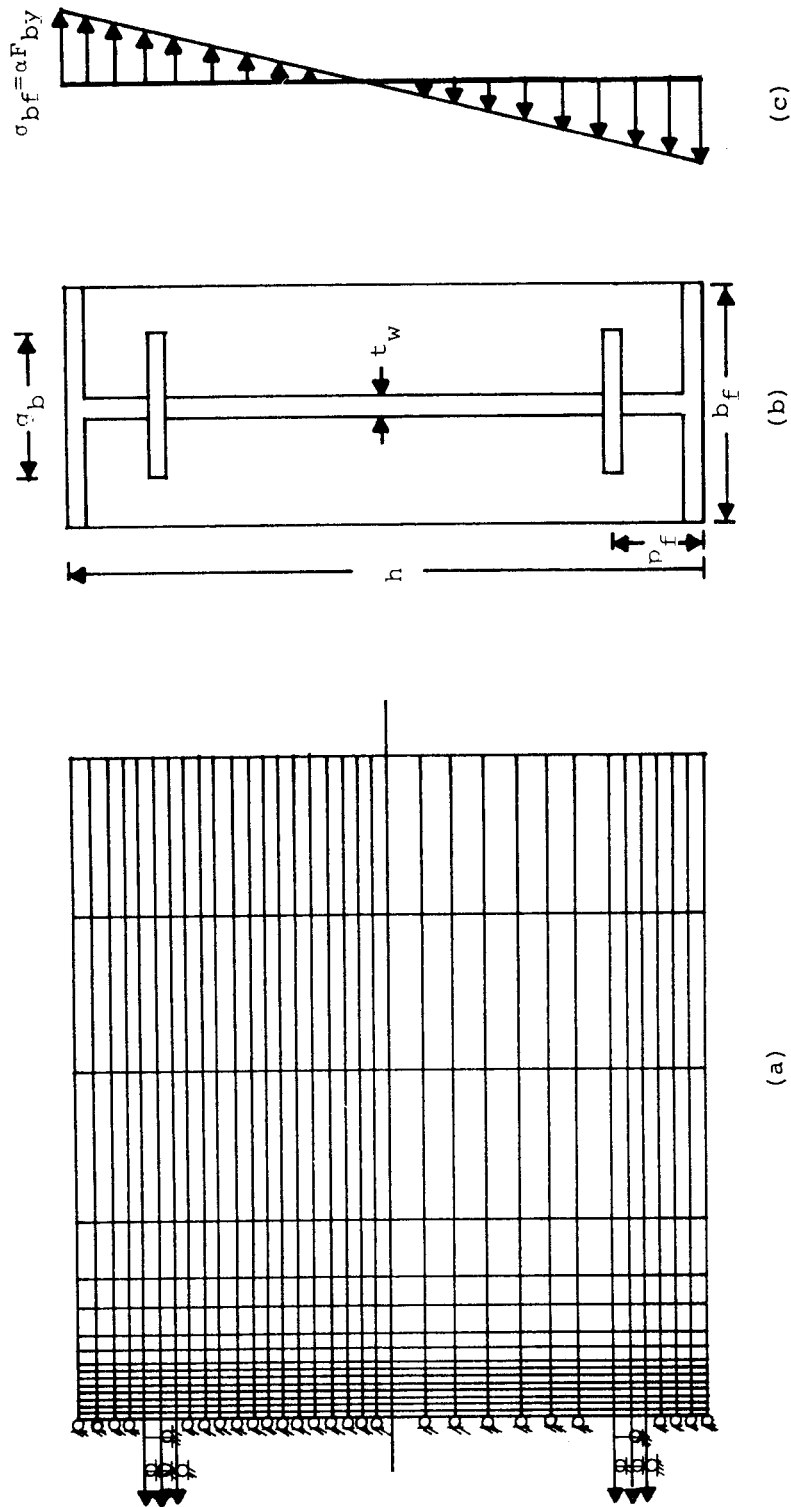


Fig. 2. Two-dimensional finite element mesh configuration. (a) Typical 2-D mesh configuration. (b) Section. (c) Assumed stress distribution.

and by
as show
bolt are
(in a re
tension
one-thi
The he
bolt di
hybrid
1252 d
To
relatio
to be e
bi-line
the ef
distor

$$\epsilon_{eff} =$$

in wh
strain
equal
value
exces
failur
If an
mess
A
bolt
Disp
then
the r
for t
subs
mon
at th
the
and
bear
W
the
sup

and by constraining the bolt centerline nodes against vertical displacement, as shown in the typical mesh configuration of Fig. 2a. For the 2-D analysis, the bolt area in a row is assumed to be uniformly spread across part of the width (in a rectangle), as shown in Fig. 2b. The equivalent bolt area for both the tension and the compression region is calculated by setting yield strength of one-third of the beam section equal to the strength of two bolts in one row. The height of the equivalent rectangular bolt area is taken to be the nominal bolt diameter. The typical 2-D mesh of Fig. 2 contains 560 rectangular hybrid plane stress elements (developed by Turner *et al.*²⁷), 626 nodes and 1252 degrees-of-freedom (d.o.f.).

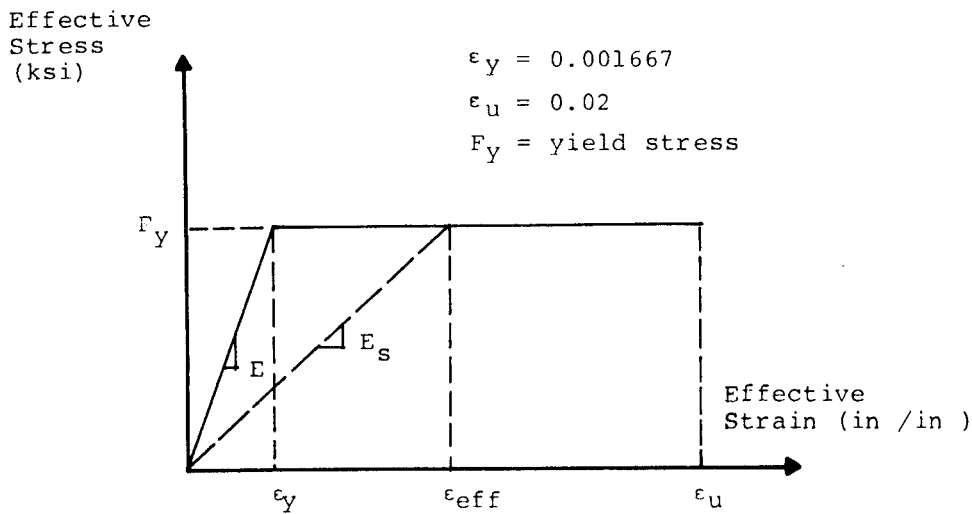
To model the non-linear material behavior, the effective stress-strain relationship for the elements of the end plate, beam flanges and web is taken to be elastic-perfectly-plastic, as shown in Fig. 3a. For bolt shank material, a bi-linear stress-strain curve is used, as shown in Fig. 3b. To check yielding, the effective strain, ϵ_{eff} , for an element was evaluated using the maximum distortion energy theory (von Mises), which gives

$$\epsilon_{\text{eff}} = \{ \sqrt{ [2(\epsilon_1 - \epsilon_2)^2 + (\epsilon_2 - \epsilon_3)^2 + (\epsilon_3 - \epsilon_1)^2] } \} / 3 \quad (1)$$

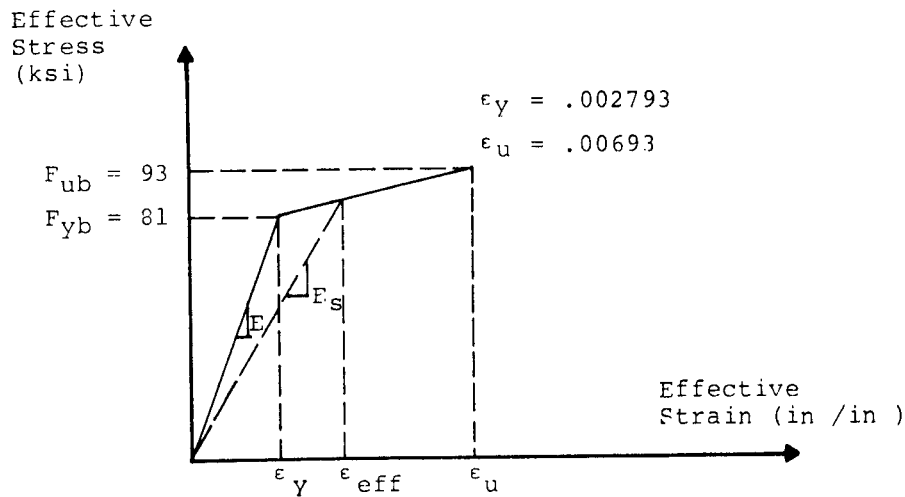
in which $\epsilon_1, \epsilon_2, \epsilon_3$ are the principal strains ($\epsilon_1 > \epsilon_2 > \epsilon_3$). If $\epsilon_{\text{eff}} \geq \epsilon_y$ (yield strain), then the element has yielded and its modulus of elasticity is reset equal to its secant value, E_s , corresponding to the respective effective strain value as indicated in Fig. 3. Failure in a plate element is said to occur due to excessive yielding if the strain reaches 0.02. For the bolt shank element, failure is said to occur due to rupture if the strain equals or exceeds 0.006 93. If any of these failure modes occurs then the execution is stopped and a message is printed defining which criterion was violated.

A typical analysis sequence is as follows. The pretension caused by the bolt tightening is first applied as forces at the end of the bolt-end nodes. Displacements of bolt nodes and the nodes at the back of the end-plate are then determined. The resulting bolt elongations and the displacements of the nodes at the back of the end-plate are applied as specified displacements for the subsequent external loadings, thus simulating the bolt tightening and subsequent interactions with the other components of the connection. The moment loading on the connection is simulated by the application of forces at the nodes on the end of the beam stub, as shown in Fig. 2c. In this figure the extreme fiber stress, σ_{bf} , is designated αF_{by} , where α is a scalar number and F_{by} is the yield stress of the beam material. The loads are applied on the beam section in increments of α varying from 0.1 to 1.0, in increments of 0.1.

When the pretension load is applied at the beginning of the analysis, all the nodes at the back of the end-plate are assumed to be in contact with the support (as shown in Fig. 2a), and the actual deformed shape is determined



(a)



(b)

Fig. 3. Idealized non-linear stress-strain curves used. (a) Idealized stress-strain diagram and secant modulus for end plate. (b) Idealized stress-strain diagram and secant modulus for A325 bolt. (1 in = 25.4 mm and 1 ksi = 6.895 MPa)

by an automated trial and error procedure. At the end of each analysis cycle, the displacements and reactions of the nodes at the back of the end plate are checked, nodes that tend to move away from the support are released; previously released nodes which moved into the support region are constrained. The process of analysis and checking support modifications is repeated until no changes occur.

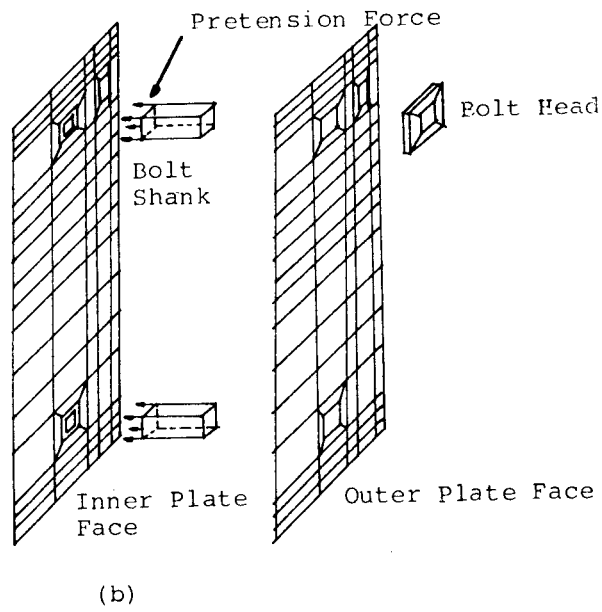
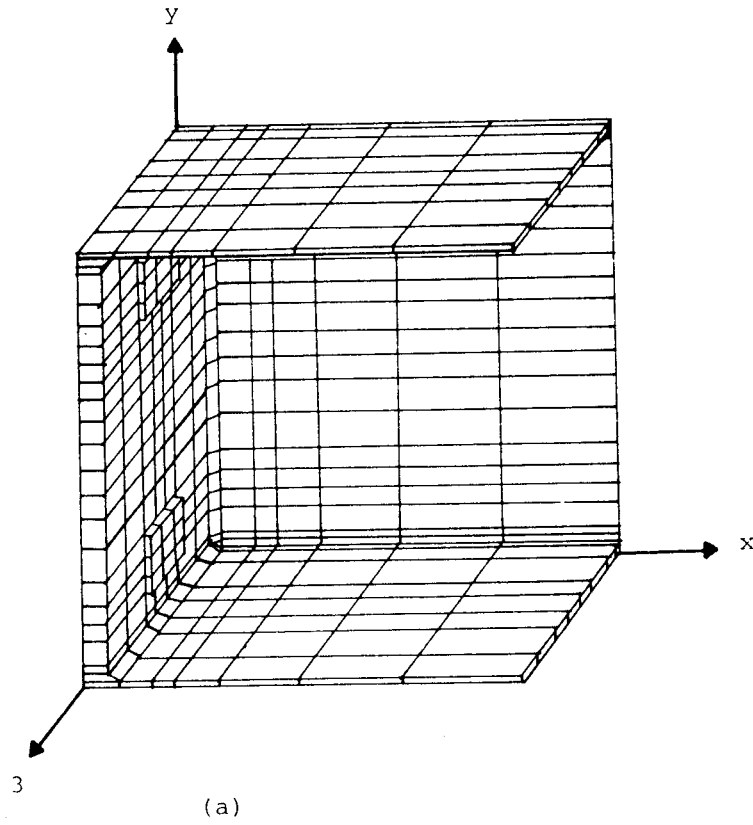


Fig. 4. Three-dimensional finite element mesh configuration. (a) Mesh configuration. (b) End-plate details.

n and
is for

ycle,
are
sed;
on-
is is

The configuration of the 3-D model used for comparison purposes is shown in Fig. 4. Due to symmetry about a plane passing through web mid-thickness, only half of the connection is considered. The most critical components of the connection, namely, the end plate, bolt shank, bolt head and the weld connecting the beam flanges with the end plate are idealized using a 33-d.o.f. 3-D subparametric element developed by Levy.²⁸ For the beam web and the weld connecting it to the end plate, eight-noded rectangular hybrid plane stress elements²⁷ are used. The influence of bolt shank has been carefully considered in this model. The nodes of the shank at the back of the end plate are distinct from those of the end plate even though they have the same coordinates (see Fig. 4b). Thus, the nodes of the bolt shank are free to move in the x -direction (axial) at the bolt pretension level. To model the necking action of the shank, one of the four nodes of the shank is allowed to move in both the y - and z -directions. The node diagonally opposite to this node is constrained in both the y - and z -directions, while one of the adjacent nodes can move only in the y -direction. The fourth node is constrained to move only in the z -direction. The bolt head area is considered as an equivalent square area equal to the actual bolt head area. The moment loading on the connection is simulated by application of forces at the end of the beam stub, as shown in Fig. 2c for the 2-D model. The typical 3-D mesh of Fig. 4 contains 546 elements, 998 nodes and 2810 d.o.f.

3 COMPARISON OF TWO-DIMENSIONAL AND THREE-DIMENSIONAL FINITE ELEMENT RESULTS

A typical 3-D finite element analysis of the mesh shown in Fig. 4 required approximately 150 minutes of Central Processor Unit (CPU) computer time for solution on an IBM 3081 computer. The 2-D finite element analysis for a similar connection required only about six minutes of CPU computer time. Thus it is obvious that the 2-D model is much more suitable than the 3-D model to develop the prediction equation for the moment-rotation behavior of the connection. The maximum end-plate separation, δ , at the level of the beam tension flange is an important parameter for the computation of the rotation ($\Theta = \delta/h$, $h =$ beam depth) of the connection. Hence it was chosen as the quantity to correlate the 3-D and 2-D results.

The 3-D finite element analyses were conducted for eight connections, which were also analyzed using the 2-D model. These connections were also experimentally tested, the results for which will be presented later on in this paper. A comparison of 3-D and 2-D results showed one dominant characteristic: the 3-D model was more flexible than the 2-D counterpart, with larger displacements and stresses. This difference in their flexibilities

Cc
 F- $\frac{3}{4}$ - $\frac{1}{2}$ -1
 F- $\frac{5}{8}$ - $\frac{1}{2}$ -1
 F- $\frac{5}{8}$ - $\frac{1}{2}$ -
 F- $\frac{3}{4}$ - $\frac{1}{2}$ -
 can b
 the p
 Th
 the c
 flexil
 the c
 of th
 were
 colu
 of $\frac{3}{4}$
 plat
 leve
 stub
 resp
 3-D
 leve
 con
 sigr
 con
 2-D
 sep

TABLE 1
Correlation of Maximum End-plate Separation Predicted by 3-D and 2-D Models

Experimental case	Load level	Φ
F- $\frac{3}{4}$ - $\frac{1}{2}$ -16	1	1.15
	2	1.07
	3	1.12
	4	1.5
F- $\frac{5}{8}$ - $\frac{1}{2}$ -10	1	1.00
	2	1.00
	3	1.01
	4	1.56
F- $\frac{5}{8}$ - $\frac{1}{2}$ -16	1	1.2
	2	1.2
	3	1.3
	4	1.6
F- $\frac{3}{4}$ - $\frac{1}{2}$ -24	1	1.2
	2	1.2
	3	1.23
	4	1.51

can be attributed to the additional constraints imposed on the 2-D model by the prevention of transverse variation of deformation and stresses.

The correlation factor Φ was defined as the ratio of the 3-D value of δ to the corresponding 2-D value. Since the 3-D model proved to be more flexible, the value of this factor was always greater than unity. Table 1 shows the end-plate separation relationship between 3-D and 2-D models for four of the connections analyzed. The results for the remaining four connections were within the range of values for Φ shown in Table 1. In this table, the first column F- $\frac{3}{4}$ - $\frac{1}{2}$ -16 designates a flush end-plate connection with one row of $\frac{3}{4}$ in (19 mm) diameter bolts near the tension flange, $\frac{1}{2}$ in (13 mm) end-plate thickness and 16 in (410 mm) beam depth. In the second column, load levels 1, 2, 3 and 4 correspond to the loads applied at the end of the beam stub to give an extreme beam fiber stress of $0.1F_{by}$, $0.2F_{by}$, $0.3F_{by}$ and $0.4F_{by}$, respectively. Thus based on the two failure criteria defined earlier, both the 3-D and the 2-D models predicted failure of the connection at the same load level. It can be seen from this table that the 2-D and 3-D models are more comparable at the lower load levels. At failure load level the two differed significantly. The δ predicted by the 3-D model at failure load level compared well with experimental results. Hence it was decided to use the 2-D model, with a correction factor of 1.5 applied to the maximum end-plate separation predicted at failure load level.

4 PARAMETRIC STUDY

A parametric study was conducted to determine the effect of various geometric and force related variables on the prediction of maximum end-plate separation. The primary geometric related independent variables for the 2-D model of the end-plate connection are identified as follows: t_p = thickness of the end-plate, p_t = pitch of the bolt (distance from top of the flange to the centerline of the bolt), t_w = thickness of the web, h = depth of the beam, d_b = nominal bolt diameter, b_p = width of the end plate, g = gage of the bolts (centerline distance between two bolts) and g_b = width of equivalent rectangular bolt area. As mentioned before, the variable g_b is calculated from

$$g_b = (1/3)(F_{by}/F_{yb})(A_B/d_b) \quad (2)$$

where F_{by} is the yield stress of the beam material, F_{yb} is the yield stress of the bolt material and A_B is the cross-sectional area of the beam. All other dimensions necessary in the analysis were set as functions of the primary geometric variables. The edge distance was set at the AISC recommended value of $1.75d_b$.¹ The plate width, b_p , was set equal to the beam flange width. The size of the fillet welds connecting the end plate to the beam flanges and the beam web was computed to develop the yield capacity of the two equivalent bolts. The primary force related independent variable in the parametric study was taken as M (= applied moment on the beam stub calculated from the double triangular stress distribution).

The primary geometric variables were non-dimensionalized with respect to the beam depth, h . This gave seven independent geometric parameters, called 'pi terms' as follows: $\pi_1 = t_p/h$, $\pi_2 = p_t/h$, $\pi_3 = t_w/h$, $\pi_4 = t_f/h$, $\pi_5 = b_p/h$, $\pi_6 = d_b/h$, and $\pi_7 = g_b/h$. In addition to these seven dimensionless parameters, one additional parameter to represent the bending stiffness of the end-plate was considered. This parameter was defined as

$$\pi_8 = p_t^3/b_p t_p^3 \quad (3)$$

This parameter has unit of $(\text{length})^{-1}$. The force related parameter was taken as $\pi_9 = M$. The primary concern of the parametric study is to develop a prediction equation for the end-plate separation, so only one dependent variable was chosen, defined as $\pi_a = \delta$, the maximum end-plate separation.

To conduct the parametric study, it was decided to limit the geometric variables to practical ranges based on usual detailing practices, as given in Table 2. Based on the ranges of variables defined in this table, the following procedure was adopted to select the beam dimensions:

- (1) Four values of beam depth, h , were selected: 10 in (254 mm), 16 in (410 mm), 24 in (615 mm) and 30 in (770 mm).

TABLE 2
Practical Ranges for Various Geometric Parameters (in)

Parameter	Low	Intermediate	High
g	$2\frac{1}{4}$	$2\frac{3}{4}$	$3\frac{1}{2}$
d_b	$\frac{5}{8}$	$\frac{3}{4}$	1
p_f	$1\frac{1}{8}$	$1\frac{3}{4}$	$2\frac{1}{2}$
b_p	5	7	10
t_p	$\frac{5}{16}$	$\frac{1}{2}$	$\frac{3}{4}$
t_f	0.18	0.375	0.50
t_w	0.10	0.1875	0.25
h	10	24	30

1 in = 25.4 mm

- (2) For each value of h , four values of beam flange width, $b_f (= b_p)$, were selected: $h/6$, $h/5$, $h/4$ and $h/3$, with the limitation that $b_f \geq 2$ in (5 mm).
- (3) For each value of b_f , four values of flange thickness, t_f , were selected: $b_f/35$, $b_f/26$, $b_f/16$ and $b_f/6$, with the limitation that $t_f \geq 0.1$ in (0.25 mm).
- (4) For each value of h , four values of web thickness, t_w , were selected: $h/160$, $h/153$, $h/107$ and $h/180$, but with the limitation that $t_w \geq 0.1$ in (0.25 mm).

Based on this procedure, a total of 256 different beam cross sections were chosen which would fall within the range of the variables given in Table 2. Since it would have been too costly to perform 2-D finite element analyses for all the 256, it was decided that only fifty beam cross sections would be used in the analysis. A regression analysis procedure was then employed to develop the desired prediction equation for π_a . The following automated procedure was used to select these fifty cases:

- (1) The value of yield moment, $M_y (= SF_{by}$, where S = elastic section modulus), was calculated for all the 256 beam cross sections.
- (2) Choose the number of beam cross sections, say n , to be considered in the study. Here, $n = 50$ was used.
- (3) Compute a moment interval, $\Delta M = ((M_y)_{\max} - (M_y)_{\min})/n$, where $(M_y)_{\max}$ and $(M_y)_{\min}$ are the maximum and minimum value, respectively, of the yield moment computed in step 1.
- (4) For each case, the beam cross section is chosen such that its moment-carrying capacity, M_m , is given by

$$M_m = (M_y)_{\min} + (m - 1)\Delta M \leq (M_y)_{\max} \quad \text{for } m = 1, 2, \dots, n \quad (4)$$

For each of the aforementioned fifty cases selected, t_p and d_b were computed from the expressions developed by Srouji²¹ based on yield line theory. As mentioned earlier, for each of these fifty connections selected, the load level was varied from the zero initial value, corresponding to the bolt pre-tension acting alone, to a level producing the extreme fiber stress in the beam material equal to αF_{by} , where α was varied from 0.1 to 1.0, in increments of 0.1. The finite element analysis was terminated either if the connection failed or if $\alpha = 1.0$, whichever occurred first.

5 PREDICTION EQUATION

The 2-D finite element results obtained for maximum end-plate separation for the fifty connections selected were statistically analyzed using the multiple regression analysis computer program SAS.²⁹ The prediction equation obtained was

$$\pi_a = e^{-8.336} \pi_1^{7.620} \pi_2^{-6.932} \pi_3^{-0.501} \pi_4^{-0.032} \pi_5^{2.885} \pi_6^{-0.849} \pi_7^{-0.519} \pi_8^{3.053} \pi_9^{1.356} \quad (5)$$

The coefficient of multiple determination, i.e. R^2 , for this regression analysis was 0.94, indicating that 94% of the variations in the data can be explained by the prediction equation (eqn (5)).

The 2-D value of the end-plate separation predicted by eqn (5) must be multiplied by the (3-D/2-D) correlation factor of 1.5 to obtain the practical estimate of the end-plate separation, δ , i.e.

$$\delta = 1.5\pi_a \quad (6)$$

The rotation, Θ , of the flush end-plate connection at any load level can be found from the following expression

$$\Theta = \frac{\delta}{h} \quad (7)$$

Substituting eqns (5) and (6) into eqn (7) and expressing the 'pi terms' in terms of the geometric variables defining them, gives

$$\Theta = CM^\beta \quad (8)$$

where

$$C = (359 \times 10^{-6}) (p_f)^{2.227} (h)^{-2.616} (t_w)^{-0.501} (t_f)^{-0.038} (d_b)^{-0.849} (g_b)^{-0.519} (b_p)^{-0.218} (t_p)^{-1.539} \quad (9)$$

is a coefficient dependent on the end-plate thickness, beam dimensions, bolt diameter and pitch of the tension bolt. The value β for the single bolt row

flush e
Expre

$M =$

where
(10) f

To ve
eight
failur
colun
cond
finite
with
was r
legs o
strain
calip
plan

Th
men
were
dicti
for a
end-
for t
eigh
we
sepa
The
sepa
vers
test
valu
Tab
0.01
(0.2
allo
con

flush end-plate was found to be to 1.356 from the regression analysis results. Expressing moment in terms of rotation, eqn (8) gives

$$M = C' \Theta^{1/\beta} \quad (10)$$

where $C' = 1/C$. It should be noted that the units used in eqns (8), (9) and (10) for length is inches (in) and for moment is kip-ft.

6 EXPERIMENTAL VERIFICATION

To verify the analytical procedure and the prediction equation so obtained, eight flush end-plate connections were tested under increasing loads up to failure. Table 3 lists the nominal geometry of the specimens tested. The last column in Table 3 gives yield stress values (F_y) obtained from coupon tests conducted on the end-plate material. This yield stress value was used in the finite element analysis. Each specimen was subjected to moment alone, without shear, by a symmetric two-point loading. The end-plate separation was measured by means of caliper gages. A spring was inserted between two legs of the caliper to keep the tips pressed against the two end-plate faces. A strain gage was mounted on the standard caliper spring and the modified caliper was calibrated prior to use. Three caliper gages were used, one at the plane of the beam section webs and one near each edge of the end-plates.

The moment versus end-plate separation plots obtained from experimental tests and 3-D finite element results were compared. These results were also compared with the corresponding values obtained from the prediction equation (eqn (6)). Table 4 illustrates the results obtained at failure for all the eight connections, whereas, Fig. 5 illustrates the moment versus end-plate plots obtained for two connections. Similar plots were obtained for the other six connections. Based on 3-D finite element analyses, all the eight test specimens failed due to excessive yielding in the end-plate (i.e. when strain ≥ 0.02). In column 3 of Table 4 the corresponding end-plate separation at failure, as obtained from 3-D finite element results, is given. The experimentally observed moment corresponding to the end-plate separation listed in column 3 of Table 4, was obtained from the moment versus end-plate separation variation for the connection plotted from the test results. These values are listed in column 4 of Table 4. Based on the values for maximum end-plate separation at failure reported in column 3 of Table 4, it can be seen that this value varies between 0.0087 in (0.221 mm) to 0.014 07 in (0.3574 mm), giving an average value of about 0.01 in (0.254 mm). Adopting a value of 0.01 in (0.254 mm) for the maximum allowable end-plate separation, the maximum allowable moment for a connection can be calculated from the prediction equations, eqns (5) and

TABLE 3
Two-bolt Flush End-plate Parameters

Test no.	Test designation	Bolt diameter d_b (in)	End-plate thickness t_p (in)	Beam depth h (in)	Flange width b_f (in)	Pitch P_f (in)	Gage g (in)	Yield stress (ksi)
1	F1- $\frac{3}{4}$ - $\frac{1}{2}$ -16	$\frac{3}{4}$	$\frac{1}{2}$ (0.505)	16	6	$1\frac{1}{2}$	$3\frac{1}{2}$	55.48
2	F1- $\frac{3}{4}$ - $\frac{3}{8}$ -16	$\frac{3}{4}$	$\frac{3}{8}$ (0.383)	16	6	$1\frac{1}{2}$	$3\frac{1}{2}$	59.45
3	F1- $\frac{5}{8}$ - $\frac{1}{2}$ -16	$\frac{5}{8}$	$\frac{1}{2}$ (0.508)	16	6	$1\frac{1}{8}$	$3\frac{3}{4}$	53.98
4	F1- $\frac{5}{8}$ - $\frac{3}{8}$ -16	$\frac{5}{8}$	$\frac{3}{8}$ (0.385)	16	6	$1\frac{3}{8}$	$2\frac{3}{4}$	56.95
5	F1- $\frac{5}{8}$ - $\frac{3}{8}$ -10	$\frac{5}{8}$	$\frac{3}{8}$ (0.384)	10	5	$1\frac{1}{4}$	$2\frac{1}{4}$	51.90
6	F1- $\frac{5}{8}$ - $\frac{1}{2}$ -10	$\frac{5}{8}$	$\frac{1}{2}$ (0.506)	10	5	$1\frac{1}{2}$	3	55.80
7	F1- $\frac{3}{4}$ - $\frac{1}{2}$ -24A	$\frac{3}{4}$	$\frac{1}{2}$ (0.504)	24	6	$1\frac{3}{4}$	$3\frac{1}{4}$	57.53
8	F1- $\frac{3}{4}$ - $\frac{1}{2}$ -24B	$\frac{3}{4}$	$\frac{1}{2}$ (0.502)	24	6	$1\frac{3}{8}$	$2\frac{3}{4}$	57.53

Flange and web thicknesses for all tests were $\frac{1}{4}$ in; (0. xxx) indicates measured thickness; 1 in = 25.4 mm; and 1 ksi = 6.895 MPa

TABLE 4
Comparison of Maximum Applied Moment Between Experimental, Finite Element and Predicted Values for Maximum End-plate Separation

Test no. (1)	Test designation (2)	δ (in) (3)	Maximum applied moment (kip-ft)				Ratios	
			Experimental (4)	F.E.M. (5)	Predicted (6)	F.E.M. Experimental (7)	Predicted Experimental (8)	Predicted F.E.M. (9)
1	F- $\frac{3}{4}$ - $\frac{1}{2}$ -16	0.012 0	59.0	67.73	71.00	1.14	1.20	0.95
2	F- $\frac{3}{4}$ - $\frac{3}{8}$ -16	0.009 4	39.0	41.26	44.00	1.06	1.12	0.94
3	F- $\frac{5}{8}$ - $\frac{1}{2}$ -16	0.014 07	54.0	68.77	54.00	1.27	1.00	1.27
4	F- $\frac{5}{8}$ - $\frac{3}{4}$ -16	0.011 6	52.0	55.02	56.00	1.06	1.07	0.93
5	F- $\frac{5}{8}$ - $\frac{3}{8}$ -10	0.008 7	21.0	25.2	20.00	1.20	0.95	1.26
6	F- $\frac{5}{8}$ - $\frac{1}{2}$ -10	0.009 5	24.19	31.67	28.84	1.30	1.19	1.10
7	F- $\frac{3}{4}$ - $\frac{1}{2}$ -24A	0.011 52	99.0	122.30	102.00	1.23	1.03	1.20
8	F- $\frac{3}{4}$ - $\frac{1}{2}$ -24B	0.010	111.00	122.30	130.00	1.10	1.17	0.94

F.E.M. means finite element method results; 1 in = 25.4 mm; and 1 kip-ft = 1.356 kN m

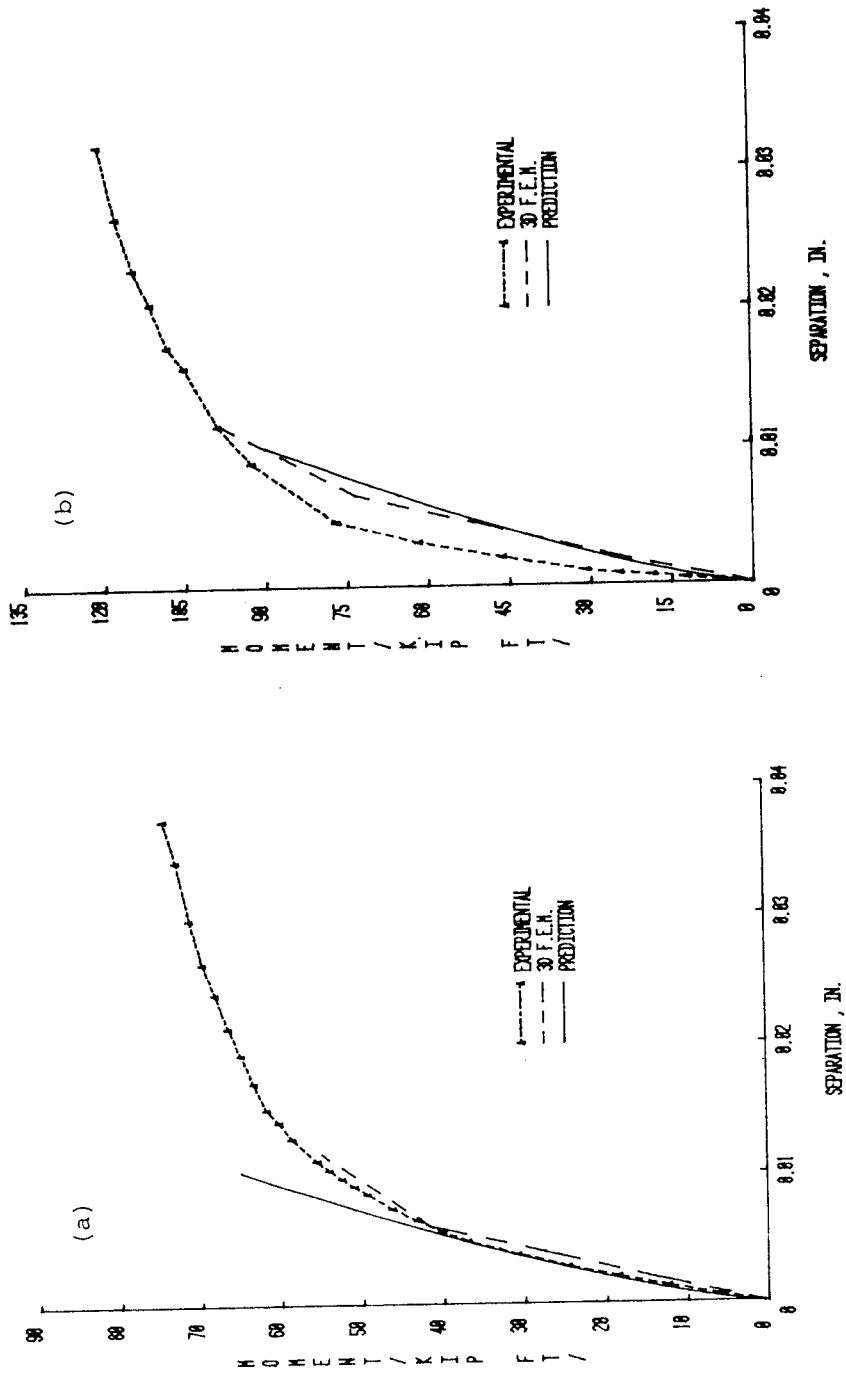


Fig. 5. Comparison of finite element (F.E.M.) analysis, prediction equation and experimental results. (a) Moment versus end-plate separation for F-1/2-16. (b) Moment versus end-plate separation for F-3/4-24A. (1 in = 25.4 mm and 1 kip-ft = 1.356 kN m)

(6), b
the e
Based
the fo
exper
betw
withi
and t
maxi
withi
prob
eqn (
bolts

In th
(ana
finite
has l
from
was
stud

The
and
ackr
don
grac

- 1.
- 2.
- 3.

(6), by setting $\delta = 0.01$ in (0.254 mm). The moment values so obtained for the eight test specimen geometrics are indicated in column 6 of Table 4. Based on the results presented in columns 7, 8 and 9, respectively, of Table 4 the following is concluded: the difference between 3-D finite element and experimental results lies within the range +6% to +30%; the difference between predicted (i.e. from eqns (5) and (6)) and experimental results lies within the range -5% to 20% (negative implying lesser predicted value); and the difference between predicted maximum applied moment and the maximum applied moment based on the 3-D finite element results lies within the range -6% to 27%. In view of the complexities involved in the problem, these comparisons show that the moment-rotation relationship, eqn (10), developed for the flush end-plate connection with a single row of bolts in the tension region, may be considered to be quite adequate.

7 CONCLUSION

In this paper, a methodology to develop the moment-rotation relationship (analytically) for a steel bolted end-plate connection has been presented. The finite element method was used as a tool to analyze a typical connection and has been validated by comparing the analytical results with those obtained from physical tests of a few selected specimens. Although the methodology was developed for a flush end-plate connection, it can also be extended to study the behavior of other types of symmetrical steel bolted connections.

ACKNOWLEDGEMENTS

The financial assistance of the Metal Building Manufacturers Association and the American Institute of Steel Construction for the project is gratefully acknowledged. The computer center of the University of Oklahoma donated valuable computational services. The assistance of Ramzi Srouji, graduate student, in conducting the experimental tests is acknowledged.

REFERENCES

1. AISC, *Manual of Steel Construction*, 8th edn, Chicago, American Institute of Steel Construction, 1980.
2. Wilson, W. M. and Moore, H. F., Tests to determine the rigidity of riveted joints of steel structures, *Bulletin No. 104*, Engineering Experimental Station, University of Illinois, Urbana, Illinois, USA, 1917.
3. Rathbun, J. C., Elastic properties of riveted connections, *Transactions*, **101**, Paper No. 1933 (1986) 24-7.

4. Douty, R. T. and McGuire, W., High-strength bolted moment connections, *J. Struct. Div., ASCE*, **91**, No. ST2 (April 1965) 101–28.
5. AISC, *Manual of Steel Construction*, 7th edn, New York, American Institute of Steel Construction, 1969.
6. Kato, B. and McGuire, W., Analysis of T-stub flange-to-column connections, *J. Struct. Div., ASCE*, **99**, No. ST5 (May 1973) 865–88.
7. Nair, R. S., Birkemore, P. C. and Munse, W. S., High-strength bolts subject to tension and prying, *J. Struct. Div., ASCE*, **100**, No. ST2, (February 1974) 351–72.
8. Fisher, J. W. and Struik, J. H. A., *Guide to Design Criteria for Bolted and Riveted Joints*, New York, John Wiley and Sons, 1974, chapters 16–18.
9. Zoetemeijer, P., A design method for the tension side of statically loaded, bolted beam-to-column connections, *Heron*, **20**, No. 1 (1974) 1–59.
10. Mann, A. P. and Morris, L. J., Limit design of extended end-plate connections, *J. Struct. Div., ASCE*, **105**, No. ST3 (March 1979) 511–26.
11. Kennedy, N. A., Vinnakota, S. and Sherbourne, A. N., 'The split-tee-analogy in bolted splices and beam-to-column connections', *Joints in Structural Steelwork*, Proceedings of the International Conference on Joints in Steelwork held at Middlesbrough, Cleveland, New York, John Wiley and Sons 1981, pp. 2·138–2·157.
12. Krishnamurthy, N., Fresh look at bolted end-plate behavior and design, *Engineering Journal, AISC*, **15**, No. 2, 2nd qtr, (1978) 39–49.
13. Krishnamurthy, N., *Analytical Investigation of Bolted Stiffened Tee-Stubs*, Report No. CE-MBMA-1902, Department of Civil Engineering, Vanderbilt University, Nashville, Tennessee, USA, 1978.
14. Tarpy, T. X., Jr. and Cardinal, J. W., 'Behavior of semi-rigid beam-to-column end-plate connections', *Joints in Structural Steelwork*, Proceedings of the International Conference on Joints in Steelwork held at Middlesbrough, Cleveland, New York, John Wiley and Sons 1981.
15. Ahuja, V., 'Analysis of stiffened end-plate connections using the finite-element method', a thesis submitted in partial fulfillment of the requirements for the degree of Master of Science, University of Oklahoma, USA, 1982.
16. Ghassemeih, M., 'Inelastic finite element analysis of stiffened end-plate connections', a thesis submitted to in partial fulfillment of the requirements for the degree of Master of Science, University of Oklahoma, Norman, Oklahoma, USA, 1983.
17. Hendrick, R. A., 'Column strength at end-plate connections', a thesis submitted in partial fulfillment of the requirements for the degree of Master of Science, University of Oklahoma, USA, 1983.
18. Parker, J. A. and Morris, L. J., A limit state design method for tension region of bolted beam-column connections, *The Structural Engineer*, **5**, No. 10 (October 1977).
19. Blockley, D. I., *The Design of Single-Story Pitched Roof Portal Frames*, BCSA Brochure, 1980.
20. Zoetermeijer, P., 'Semi-rigid bolted beam-to-column connections with stiffened column flanges and flush end-plate', *Joints in Structural Steelwork*, Proceedings of the International Conference on Joints in Steelwork held at Middlesbrough, Cleveland, New York, John Wiley and Sons, 1981, pp. 2·99–2·118.

21. Sr
pr
de
22. D
(ir
23. N
C
19
24. P
co
C
Y
25. K
fu
C
U
26. P
N
27. T
J
28. L
N
29. D
19

21. Srouji, R., 'Yield-line analysis of end-plate connections with bolt force predictions', a thesis submitted in partial fulfillment of the requirements for the degree of Master of Science, University of Oklahoma, USA, 1983.
22. DSTV/DAST, *Moment and Plate Connections with HSFG Bolts*, IHE 1, 1978 (in German).
23. Norme Francaise Enregistree, Metal Construction, *Joining by Means Bolts Controlled Tightening, Structural Requirements and Checking of Jointing*, NF, 1979, pp. 22-460 (in French).
24. Phillips, J. and Parker, J. A., 'The effect of plate thickness on flush end-plate connections', *Joints in Structural Steelwork*, Proceedings of the International Conference on Joints in Steelwork held at Middlesbrough, Cleveland, New York, John Wiley and Sons 1981, pp. 6.77-6.92.
25. Krishnamurthy, N., *Two-dimensional finite element analysis of extended and flush connections with multiple rows of bolts*, Report to AISC and MBMA, No. CE-AISC-MBMA-6, Department of Civil Engineering, Auburn University, USA, March 1975.
26. Patel, K. and Chen, W. F., Analysis of fully bolted moment connection using NONSA, *Computers and Structures*, 21, No. 3 (1985) 505-11.
27. Turner, M. H. *et al.*, Stiffness and deflection analysis of complex structures, *Journal of Aeronautical Science*, No. 23 (September 1956) 815-24.
28. Levy, S., *3-D Isoparametric Finite Element Program*, Report No. 71-C-191, New York, General Electric Company, June 1971.
29. Draper, S., *Applied Regression Analysis*, New York, John Wiley and Sons, 1981.